



## Influence of rock specimen diameter size on the ultrasonic pulse velocity and dynamic elastic constants

Amin Jamshidi <sup>1,\*</sup>, Rasool Yazarloo <sup>2</sup>

<sup>1</sup> Department of Geology, Faculty of Basic Sciences, Lorestan University, Khorramabad, Islamic Republic of Iran

<sup>2</sup> Department of civil engineering, Gonbad Kavoods Branch, Islamic Azad University, Gonbad Kavoods, Islamic Republic of Iran

Received: 13 January 2021, Revised: 11 March 2021, Accepted: 17 March 2021

© University of Tehran

### Abstract

The ultrasonic pulse velocity including P-wave ( $V_p$ ) and S-wave ( $V_s$ ) velocity and elastic constants including the elastic modulus ( $E$ ) and Poisson's ratio ( $\nu$ ) are among most important parameters for estimating the strength and deformability properties of rocks. The specimen diameter size is one of the main factors that influence  $V_p$ ,  $V_s$ ,  $E$  and  $\nu$ . This study presents the influence of specimen diameter size on the  $V_p$ ,  $V_s$ ,  $E$  and  $\nu$  of sandstones. Moreover, we have investigated the accuracy of porosity ( $n$ ) for estimating the  $V_p$ ,  $V_s$ ,  $E$  and  $\nu$  at different diameters size. For this purpose, 10 sandstone samples were collected and core specimens with a diameters size of 24, 40, 54, 68, and 80 mm were prepared. Then, density ( $\rho$ ),  $n$ ,  $V_p$ ,  $V_s$ ,  $E$  and  $\nu$  of sandstones were determined. It is concluded that the specimen diameter size has a significant influence  $V_p$ ,  $V_s$ ,  $E$  and  $\nu$ . Moreover, the results showed that  $n$  is in good accuracy for estimating the  $V_p$ ,  $V_s$  and  $E$ , while there are no meaningful correlations between  $\nu$  with  $n$ .

**Keywords:** P-Wave Velocity, S-Wave Velocity, Elastic Modulus, Poisson's Ratio, Specimen Diameter Size.

### Introduction

P-wave and S-wave velocity tests ( $V_p$  and  $V_s$ ), which are non-destructive, cost effective and easy to apply, have been used for many years in mining, geotechnical and civil engineering such as quarrying, rock slopes, underground opening, blasting and ripping (Ercikdi et al., 2014; Yilmaz et al., 2014; Ayaz et al., 2015; Eskisar et al., 2015; Özkan & Yayla 2016; Wua et al., 2016; Jamshidi & Torabi-Kaveh, 2020). On the other hand, elastic constants are important to use in planning and design of underground structures as well as in any numerical simulation of excavation. Among them, elastic modulus ( $E$ ) and Poisson's ratio ( $\nu$ ) are very critical, cumbersome, and useful parameters, due to their application in tunnel design, drilling and blasting of rock, slope stability, pillar design, support design, embankments, and many other civil and mining operations (Khandelwal & Singh, 2011). Moreover,  $E$  and  $\nu$  are the parameters determining the deformability of the material under applied loads, making these as essential parameters for any structural elements (Eissa & Kazi, 1988; Ciccotti & Mulargia, 2004; Al-Shayea, 2014). These parameters can be obtained from non-destructive testing: typically using results obtained from tests measuring the propagation velocity of  $V_p$  and  $V_s$ , also called the dynamic elastic constants (King, 1983; Eissa & Kazi, 1988; Christaras et al., 1994; Ameen et al., 2009; Najibi et al., 2015).

\* Corresponding author e-mail: jamshidi.am@lu.ac.ir

Some researchers have investigated the correlations among the  $V_p$ ,  $V_s$ ,  $E$  and  $\nu$  of rocks (Ocak & Seker, 2012; Martinez-Martinez et al., 2012; Brotons et al., 2014). Also various researchers have studied a number of factors that influence the  $V_p$ ,  $V_s$ ,  $E$  and  $\nu$  (Fahy & Guccione, 1979; Ulusay et al., 1994; Koncagül & Santi, 1999; Yilmaz, 2007). The important factors are rock type, texture, density, grain size and shape, porosity, anisotropy, water content, stress and temperature. In addition,  $V_p$  and  $V_s$  are influenced by the shape and size of the samples (Vasconcelos et al., 2008; Fener, 2011; Ercikdi et al., 2014; Karaman et al., 2015). However, influence specimen diameter size on  $E$  and  $\nu$  was still unknown. Moreover, although the correlations between  $V_p$ ,  $V_s$ ,  $E$  and  $\nu$  with  $n$  have been investigated for several decades, influence of specimen diameter size on correlations between those were still unknown and it should be studied further. Due to these, there is a need to better understand the influence specimen diameter size on the  $E$  and  $\nu$  and also correlations between  $V_p$ ,  $V_s$ ,  $E$  and  $\nu$  with  $n$  when specimen diameter size is considered as an affective factor on those.

This study has two main purposes: to find out the influence of specimen diameter size on  $V_p$ ,  $V_s$ ,  $E$  and  $\nu$ , and to investigate the correlations between  $V_p$ ,  $V_s$ ,  $E$  and  $\nu$  with  $n$  together with influence of specimen diameter size for 10 sandstone samples.

## Materials and methods

Ten different sandstones have been collected for this study. All of them are quarried from various outcrops of Ghasem Abad village in north Khorramabad (southwest Iran) and generally commercialized as construction materials for buildings. Figure 1 shows a geological map of the sampling area. The core specimens from sandstones were taken at different diameters of 24, 40, 54, 68 and 80 mm. The  $V_p$  and  $V_s$  tests were performed on the specimens and then  $E$  and  $\nu$  from  $V_p$  and  $V_s$  were obtained. Influence of specimen diameter size on  $V_p$ ,  $V_s$ ,  $E$  and  $\nu$  was examined. Further, the correlations between  $V_p$ ,  $V_s$ ,  $E$  and  $\nu$  with  $n$  together with influence of specimen diameter size were investigated. To obtain the purposes of the study, methodology given in Figure 2 is followed.

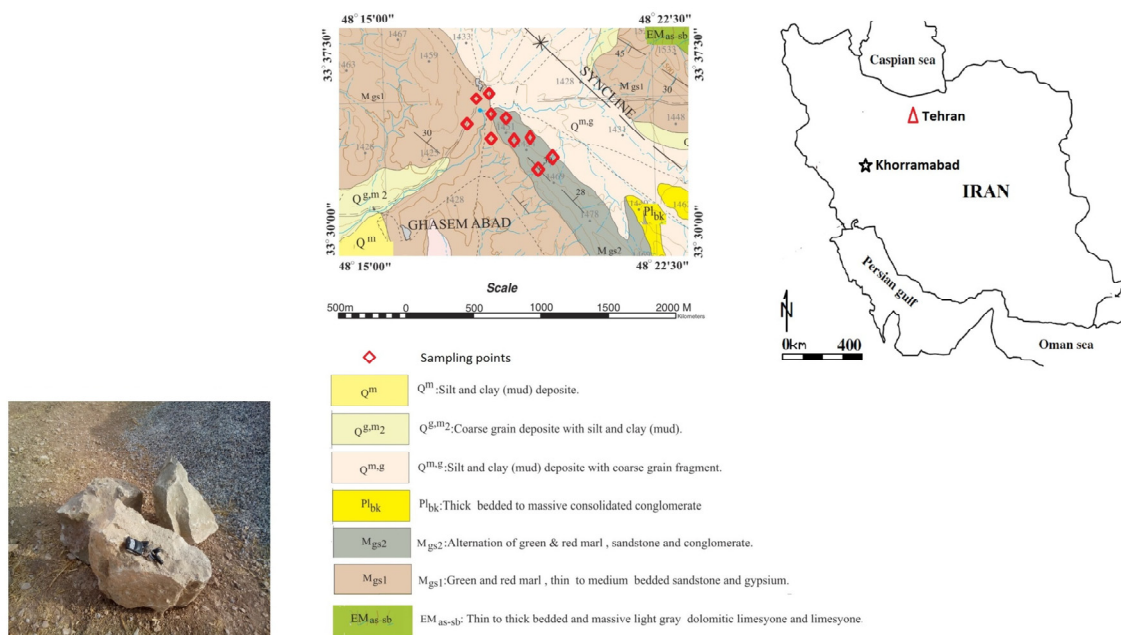


**Figure 1.** Geological map of the sampling area and the some of the block samples (Geological map of Khorramabad; 1:25000 by Zamin Danesh-e-Pars consulting engineers)

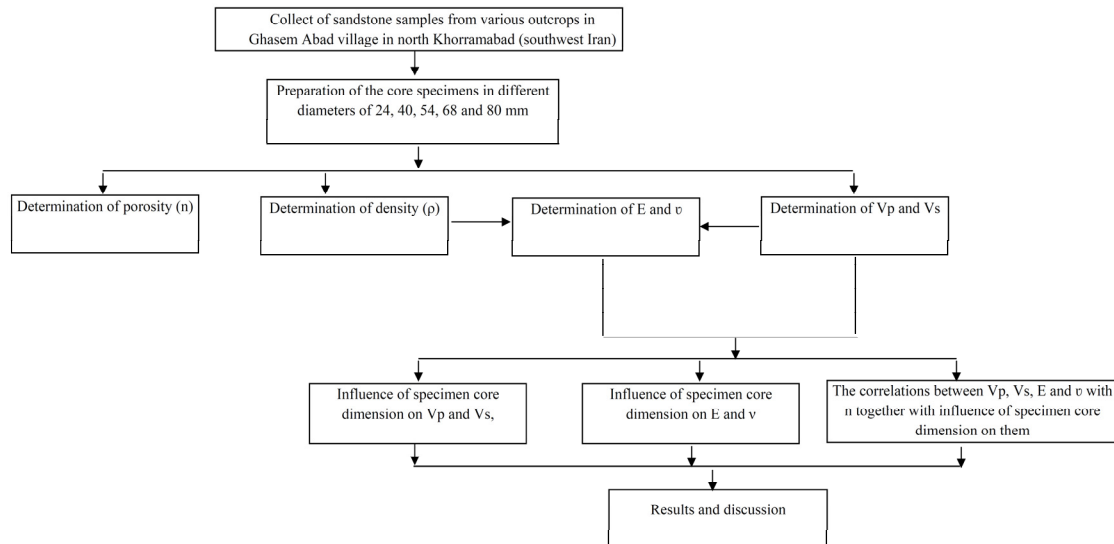


**Figure 2.** Methodology of the study

## Rock sampling

Sandstone outcrops in Ghasem Abad area of Iran were visited and representative blocks were collected to fulfill the purpose of this study. The block samples varied from  $25 \times 30 \times 40$  to  $30 \times 30 \times 45$  cm<sup>3</sup> in size. Fig. 1 shows one of the outcrops of sampling area and the some of the block samples. During the sampling, rock types having no bedding planes and fracture were selected to eliminate any anisotropy effects on the measurement as suggested in the literature (Jamshidi et al., 2021).

## Experimental studies

### *Petrographical characteristics*

Petrographical characteristics including the mineralogical composition of the grains and the cement type were investigated using an optical polarizing microscope. Fig. 3 presents a microscopic image of a tested sandstone sample. Petrographic studies under a polarized microscope show that dominant detrital framework grains of sandstone samples include rock fragments (R), feldspar (F) and quartz (Q). Other minerals include mica and accessory heavy minerals. Rock fragments is the dominating framework grain in thin sections studied (Table 1). The petrographic (modal) analysis of sandstone samples shows that the percentage range of composition of rock fragments by volume is 53.2–57.0%, feldspar 7.0–16%, quartz 0.8–4.5%, matrix (M) 4.2–9.8% and cement (C) 15.5–31.0%. The recalculated percentage frequency of the detrital framework grains shows total rock fragment varying from 70.51 to 84.77%, feldspar from 10.27 to 26.64% and quartz from 1.80 to 6.20% (Table 1). The rock fragment grains are subangular to subrounded and have straight to strongly undulose extinction. The feldspars which are mainly k-feldspars have average value of 17.42% of the total detrital framework grains. Quartz constitutes the least proportion of the framework grains. In some of sandstone samples, cement constitutes over 30% of the total rock volume. The cement is identified as silica, calcite iron oxide/detrital clay. Calcite is the cementing agent for samples from quarry along Amasiri–Okposi Road (Fig. 4a) and ferruginous iron oxide/detrital clay for samples from Ozaraukwu. There is occurrence of undulose and elongate quartz grains (Fig. 4). The fabric sandstone samples is framework–supported with mainly concavo-convex contacts. From

the recalculated framework composition of rock fragments, feldspars and quartz (Table 1), a ternary plot (QFR) for classification of Folk (1974) puts the sandstones in feldspathic litharenite field.

**Table 1.** The modal composition of the sandstone samples

Rock name	Sandstone composition					Recalculated framework composition		
	R (%)	F (%)	Q (%)	C (%)	M (%)	R (%)	F (%)	Q (%)
Sandstones 1	57.0	12.8	4.2	21.2	4.8	77.70	17.90	4.40
Sandstones 2	54.5	13.2	4.5	22.2	5.6	75.10	18.70	6.20
Sandstones 3	53.6	15.8	3.1	21.1	6.4	73.55	21.79	4.66
Sandstones 4	54.0	9.0	1.6	29.4	6.0	83.60	13.40	3.00
Sandstones 5	55.0	21.0	2.0	15.5	6.5	70.51	26.64	2.85
Sandstones 6	53.2	9.0	2.0	30.5	5.3	83.40	13.50	3.10
Sandstones 7	56.8	16.0	2.5	18.8	5.8	75.10	21.25	3.65
Sandstones 8	54.0	11.0	0.8	31.0	4.2	82.80	16.40	1.80
Sandstones 9	55.2	7.0	3.5	25.5	9.8	84.77	10.27	5.96
Sandstones 10	56.6	10.2	2.1	21.6	7.5	80.24	14.39	3.37

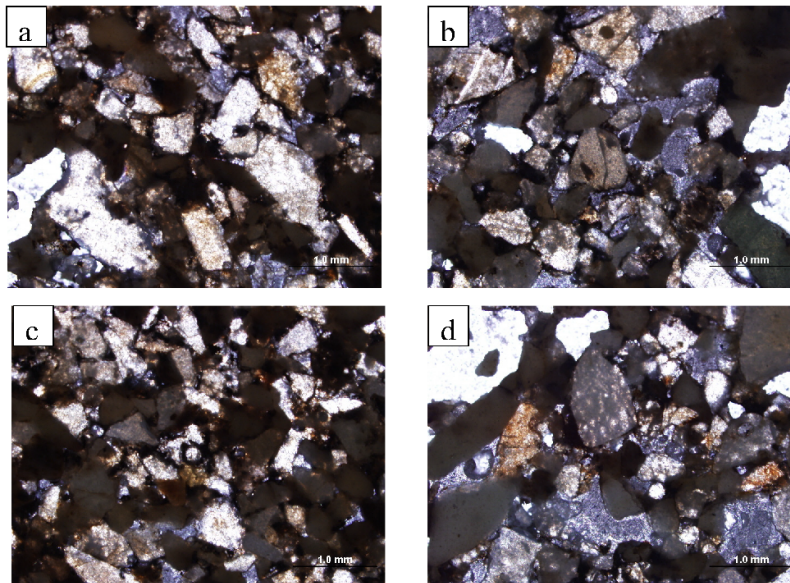


**Figure 3.** Photomicrographs some of the tested samples a) sandstone 1 b) sandstone 5 c) sandstone 6 d) sandstone 10



**Figure 4.** The ultrasonic pulse velocity testing equipment

### Density and Porosity Tests

Some physical properties of the sandstones including density ( $\rho$ ) and porosity ( $n$ ) were determined using the saturation method in accordance with ISRM (1981).  $\rho$  and  $n$  were calculated using the following relations, respectively:

$$\rho = \frac{m_s}{V} \quad (1)$$

$$n = \frac{(m_{\text{sat}} - m_s) / \rho_w}{V} \times 100 \quad (2)$$

Where,  $m_s$  is a solid mass of the specimen,  $m_{\text{sat}}$  is a surface-dry saturated mass,  $V$  is a bulk volume and  $\rho_w$  is density of water.

Five specimens from each sandstone sample were used and then the mean values were obtained. The results of these determinations are given in Table 2. Using the tests results, the sandstones are classified as rocks with moderate and high density (2.20–2.55 and 2.55–2.75 g/cm<sup>3</sup>, respectively) and low and medium porosity (1–5 and 5–15%, respectively) according to the classification suggested by Matula et al. (1979).

### $V_p$ and $V_s$ tests

The ultrasonic pulse velocity measurement system that used “Starmans-DIO1000 LF” is a rectangular electrical pulser (Fig. 4). Produce pulse is converted to a mechanical pulse by a piezoelectric transducer. The mechanical wave received at the other end of the specimen is converted back to an electrical signal which is passed through a high-pass filter, amplified by a wideband amplifier, and displayed on the screen of a dual beam oscilloscope. The pulse transmission technique of velocity measurements has been used with 63 kHz central frequency for  $V_p$  and 33 kHz for  $V_s$  transducers as an overall accuracy of the velocity measurements of about 1 % achieved.

**Table 2.** Physical properties of the sandstones under study

Rock name	Density (g/cm <sup>3</sup> )	Porosity (%)
Sandstones 1	2.48	7.44
Sandstones 2	2.72	3.17
Sandstones 3	2.43	5.65
Sandstones 4	2.69	4.19
Sandstones 5	2.66	3.97
Sandstones 6	2.46	2.64
Sandstones 7	2.55	3.32
Sandstones 8	2.47	7.20
Sandstones 9	2.51	6.26
Sandstones 10	2.42	6.03

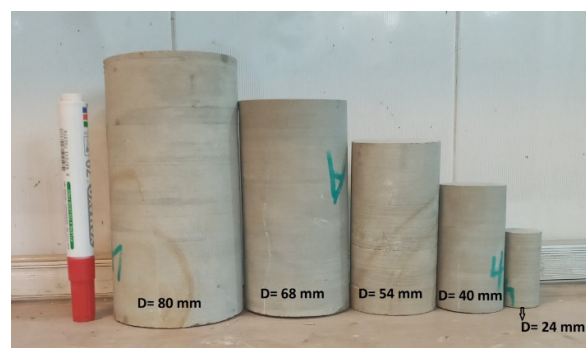


**Figure 5.** Core specimens at different diameters size (Sandstone 6)

The core specimens were taken at five different diameters from all sandstones. These diameters are 24, 40, 54, 68 and 80, with the length to diameter ratio of 2 (Fig. 5). With the help of a polishing and lapping machine, the ends of the specimens were made flat and perpendicular to the axis of the specimens within 0.05 mm in 50 mm and their sides were smoothed and polished. Then end surfaces of the core specimens covered with stiffer grease to provide a good coupling between the transducer face and the specimen surface to maximize accuracy of the transit time measurement. The  $V_p$  and  $V_s$  through the specimen was calculated from the travel time from the generator to a receiver at the opposite end. For each diameter, five specimens were prepared and their  $V_p$  and  $V_s$  were determined according to ISRM (1981). All of the core specimens used for  $V_p$  measurement were also used in the determination of  $V_s$ . The mean values of these tests are given in Table 3.

#### *Determination of E and $\nu$ using $V_p$ and $V_s$*

Two types of procedures exist for obtaining the E and  $\nu$  of rocks: destructive and non-destructive methodologies. The most widespread nondestructive procedure is the calculus of the E and  $\nu$  via  $V_p$  and  $V_s$  tests. In this study, the E and  $\nu$  are calculated by means of the following equations, respectively:

$$E = \rho V_s^2 \frac{(4V_s^2 - 3V_p^2)}{(V_s^2 - V_p^2)} \quad (3)$$

$$\nu = \frac{V_p^2 - 2V_s^2}{2V_p^2 - 2V_s^2} \quad (4)$$

Where E is the dynamic elastic modulus,  $\nu$  is the Poisson's ratio;  $V_p$  and  $V_s$  are the compressional and shear ultrasonic wave velocities, respectively; and  $\rho$  is the bulk density of the sample. The results of E and  $\nu$  measurements for sandstones having different diameters size are shown in Table 4.

## Results and discussion

#### *Influence of specimen diameter size on $V_p$ , $V_s$ , E and $\nu$*

Figures 6 and 7 graphically display the  $V_p$  and  $V_s$  of sandstones at different diameters size. When the data given in Figures 6 and 7 are examined, it is seen that increase in specimen diameter size results with decrease in the  $V_p$  and  $V_s$  values. Decrease in  $V_p$  and  $V_s$  values is initially very significant and reaching a constant velocity value at a Critical Diameter Size (CDS).

**Table 3.**  $V_p$  and  $V_s$  values of the sandstones in different diameters size

Rock name	$V_p$ (m/s)					$V_s$ (m/s)				
	24 mm	40 mm	54 mm	68 mm	80 mm	24 mm	40 mm	54 mm	68 mm	80 mm
Sandstones 1	3953	3850	3775	3643	3652	2196	2081	1956	1843	1832
Sandstones 2	5260	5026	4720	4700	4687	2802	2617	2446	2427	2425
Sandstones 3	4470	4410	4350	4206	4200	2482	2371	2262	2088	2090
Sandstones 4	5011	4899	4703	4702	4711	2792	2632	2437	2430	2437
Sandstones 5	4930	4902	4744	4734	4740	2652	2532	2372	2365	2354
Sandstones 6	5450	5400	5274	5283	5270	3054	2852	2643	2632	2611
Sandstones 7	5317	5225	5100	5096	5102	2867	2701	2451	2455	2440
Sandstones 8	4298	4210	4155	4009	4001	2398	2254	2172	2005	2013
Sandstones 9	4901	4830	4670	4568	4573	2702	2542	2390	2300	2297
Sandstones 10	4600	4260	4103	3780	3773	2501	2300	2156	1900	1891

**Table 4.** *E* and *v* values of the sandstones in different diameters size

Rock name	<i>E</i> (GPa)					<i>v</i>				
	24 mm	40 mm	54 mm	68 mm	80 mm	24 mm	40 mm	54 mm	68 mm	80 mm
Sandstones 1	30.5	27.8	25.0	22.4	22.2	0.277	0.294	0.317	0.328	0.332
Sandstones 2	55.6	49.0	42.8	42.2	42.1	0.302	0.314	0.317	0.318	0.317
Sandstones 3	38.2	35.4	32.7	28.3	28.3	0.277	0.297	0.315	0.336	0.335
Sandstones 4	53.5	48.3	42.1	41.9	42.1	0.275	0.297	0.317	0.318	0.317
Sandstones 5	48.5	45.0	39.9	39.7	39.4	0.296	0.318	0.333	0.334	0.336
Sandstones 6	58.3	52.3	45.8	45.5	44.9	0.271	0.307	0.332	0.335	0.337
Sandstones 7	54.3	49.0	41.4	41.5	41.0	0.295	0.318	0.350	0.349	0.352
Sandstones 8	36.2	32.6	30.6	26.5	26.6	0.274	0.299	0.312	0.333	0.331
Sandstones 9	47.0	42.4	37.9	35.3	35.3	0.282	0.308	0.323	0.330	0.331
Sandstones 10	39.1	33.1	29.5	23.3	23.1	0.290	0.294	0.309	0.331	0.332

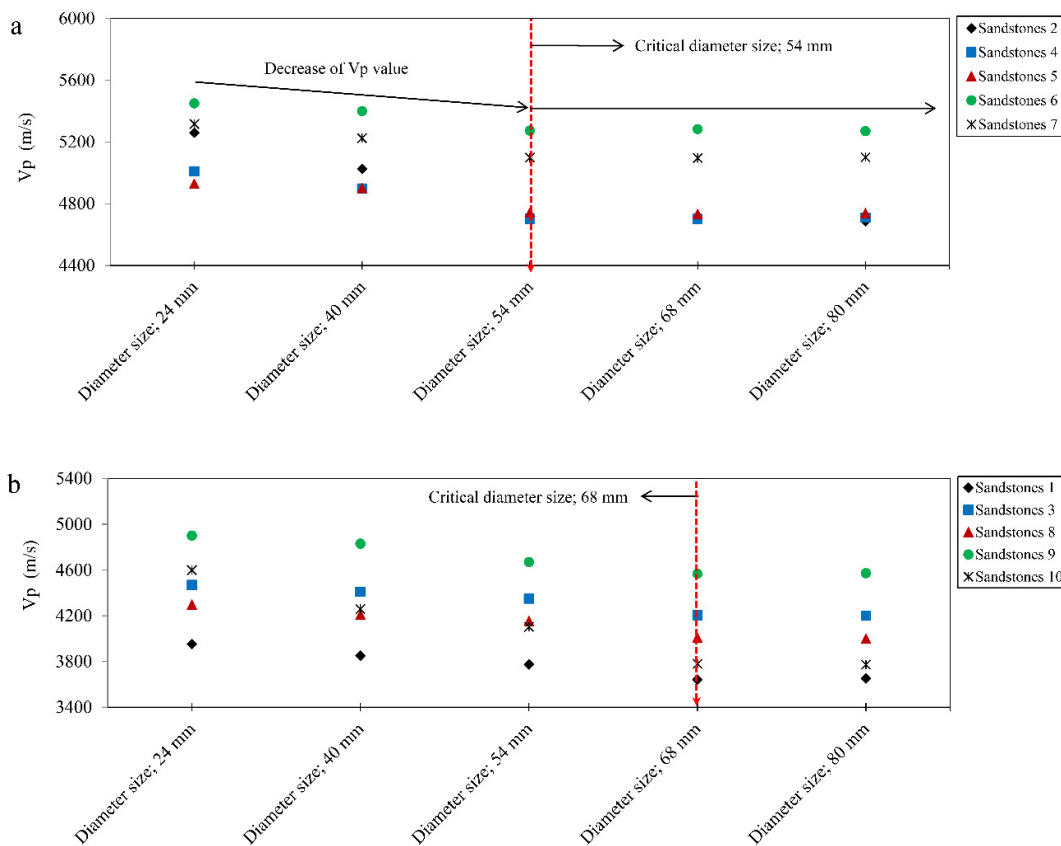


**Figure 6.** Vp values of the sandstones at different diameters size a) Sandstones with porosity lower than 5% b) Sandstones with porosity higher than 5%

For instance, the highest and lowest Vp values for the sandstone 10 were obtained for the specimens having 24 (4600 m/s) and 80 mm (3773 m/s) diameters, respectively, with a pronounced reduction of 827 m/s between these diameters. Changes in the Vp and Vs values of rocks with the increase of specimen diameter size can be due to the inherent heterogeneity in structure and composition (i.e. mineralogical or chemical or physical such as mineral grain size) of rocks and discontinuities (e.g. cracks, microcracks, etc.) that are often present in rocks (Ercikdi et al., 2016). In present study, the change of Vp is consistent with the findings of Fener’s (2011) research on the samples of tuff (Kayseri), basalt and andesite. He found an

inverse relationship between  $V_p$  and the specimen diameter. However, he only obtained the polynomial relationships between  $V_p$  and the specimen diameter for limestone, dolomite, tuff (Nevsehir) and sandstone.

In order to determine the CDS for the consistent  $V_p$  and  $V_s$  values, two lines were fitted to the data; one is an inclined line fitted to  $V_p$  and  $V_s$  data increasing with diameter size; the other is a horizontal line fitted to  $V_p$  and  $V_s$  data showing no changes with diameter size (Fig. 6a). The value at the intersection point of two lines for each sandstone is a CDS value. Porosity is one of the most important physical features controlling the ultrasonic pulse velocity. It can be seen from Table 2 that the porosity ranges of sandstones are from 2.64 to 7.44%, while the average porosity is 5%. To observe the influence of porosity on CDS, the sandstones based on average porosity were classified into two groups. The sandstones with lower and higher porosities than the average (5%) were assigned as group less porous and porous, respectively. The CDS according to Figures 6 and 7 is 54 and 68 mm for the sandstones with less porous and porous, respectively. In fact, sandstones with less porous than those with porous has less CDS. As was seen from these results, minimum diameter size of a core specimen should be at least 54 and 68 mm to attain a consistent ultrasonic pulse velocity values determination for sandstones with less porous and porous, respectively.

Studied sandstones are also classified according to their  $V_p$  values as suggested by Anon (1979 (Fig. 8) (dashed lines). As shown in this figure, sandstones with respect to the diameters size of 24, 40, 54, 68 and 80 fall into the different rocks class with moderate, high and very high velocity. For instance, sandstone 2 at the diameters size of 54, 68 and 80 fall into the rocks class with high velocity ( $V_p$  4000- 5000 m/s), whereas at a diameter size of 24 and 40, it goes into the rocks class with very high velocity ( $V_p > 5000$  m/s).

Figures 9 and 10 illustrate the  $E$  and  $\nu$  sandstones at different diameters size. It can be seen from these figures that a similar pattern with  $V_p$  and  $V_s$  (Figs. 6 and 7) was also obtained.

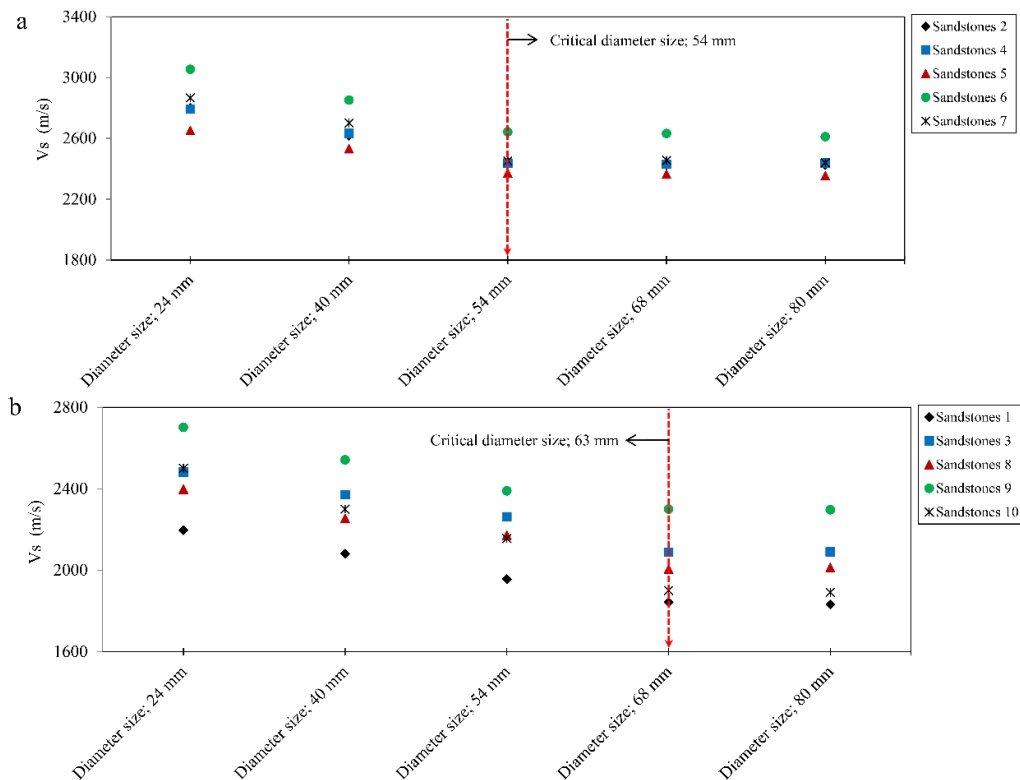


**Figure 7.**  $V_s$  values of the sandstones at different diameters size a) Sandstones with porosity lower than 5% b) Sandstones with porosity higher than 5%

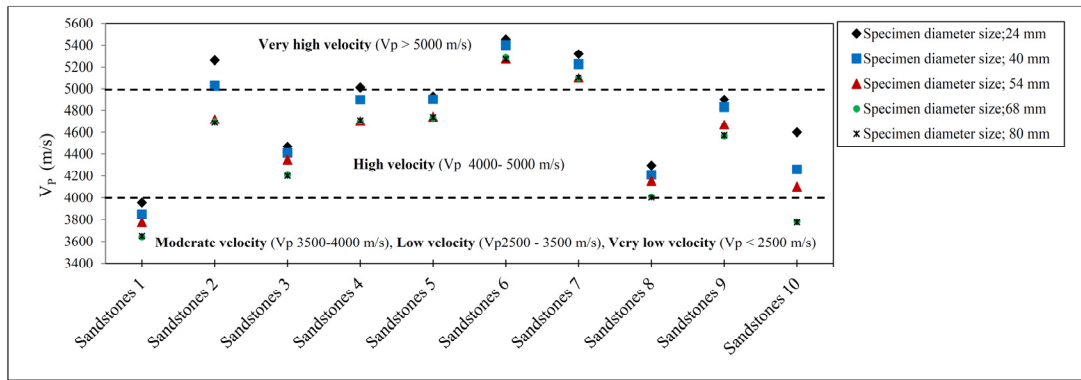


**Figure 8.** Classification of the sandstones based on  $V_p$  at different diameters size

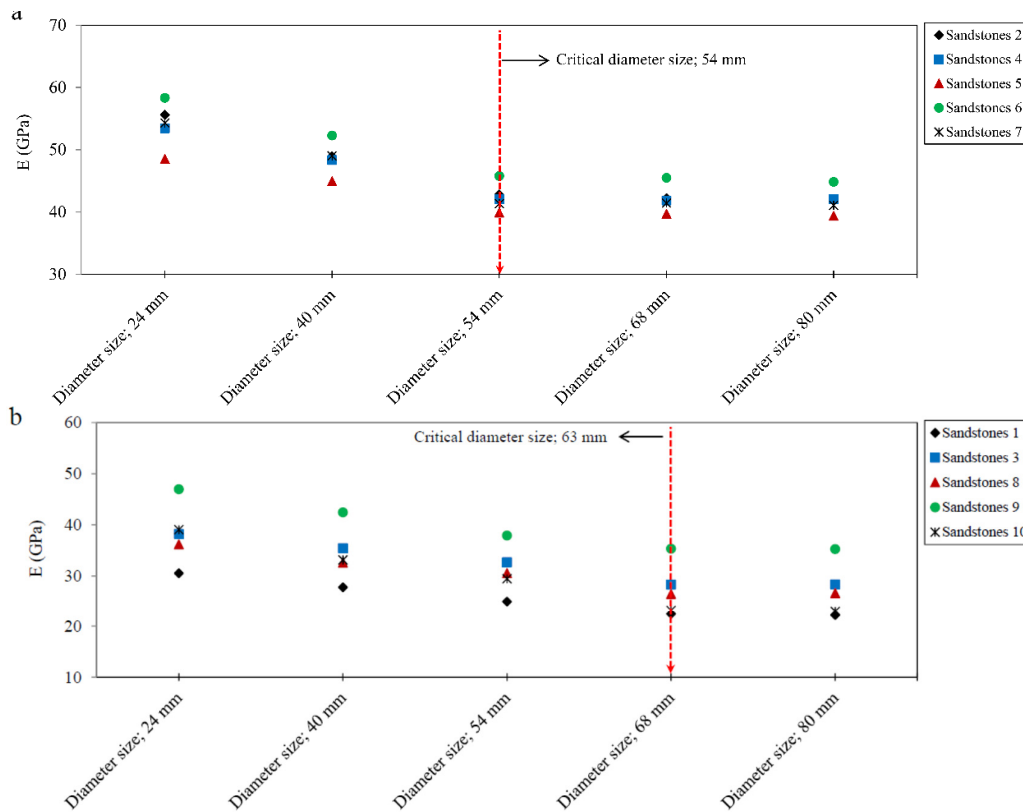


**Figure 9.** E values of the sandstones at different diameters size a) Sandstones with porosity lower than 5% b) Sandstones with porosity higher than 5%

*Correlation between  $V_p$ ,  $V_s$ , E and  $v$  with  $n$  in different specimen diameters size*

One of the most common accepted methods of investigating empirical relationships between rocks properties is regression analyses (Zalooli et al., 2017; Hashemi et al., 2018). The author this work attempted to develop the best correlation between with  $V_p$ ,  $V_s$ , E and  $v$  with  $n$  among the different diameters of specimens to attain the most reliable empirical relations. The equation of the best fit line, the 95% confidence limits and the determination coefficients ( $r^2$ ) were determined for each regression.

In figure 11, the correlations of  $V_p$  and  $V_s$  with  $n$  are presented for different diameters size. It can be seen that, in all cases, the best-fitted relations have been represented by linear regression curves.

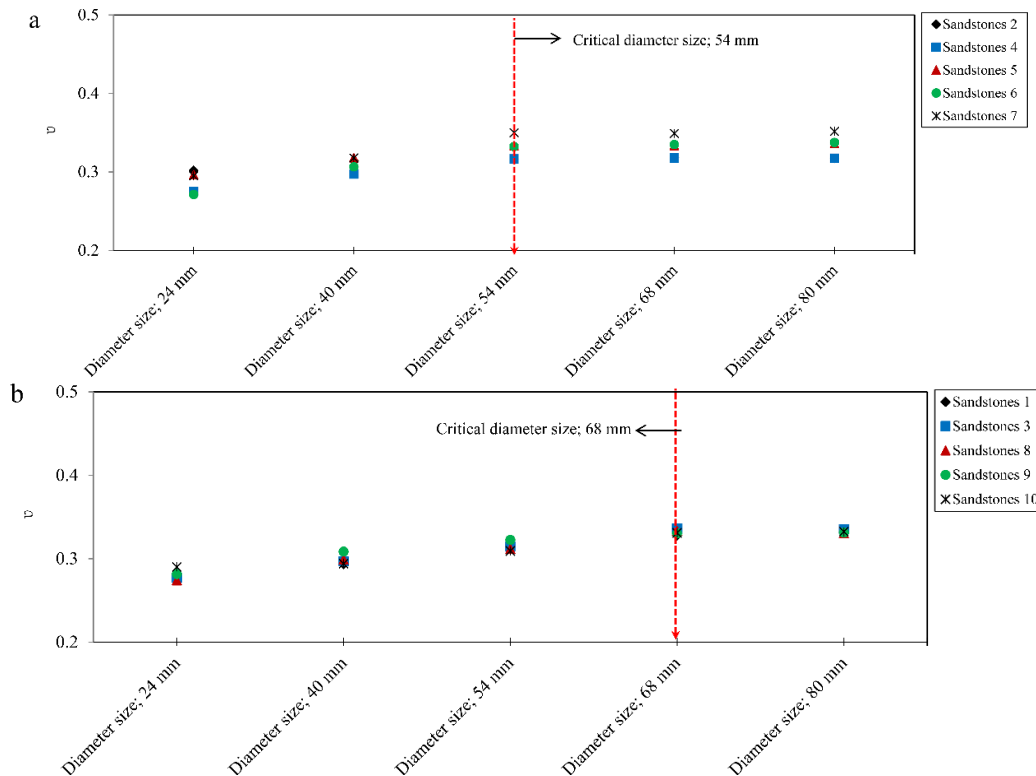


**Figure 10.**  $v$  values of the sandstones at different diameters size a) Sandstones with porosity lower than 5% b) Sandstones with porosity higher than 5%

Also, it can be concluded from figure 11 that for different diameters size, the determination coefficients ( $r^2$ ) between  $V_p$  and  $V_s$  with  $n$  are different.

In correlation between  $V_p$  and  $n$  the highest determination coefficient,  $r^2=0.86$ , was obtained for the specimen diameter of 24 mm and the lowest was for the diameter of 80 mm with  $r^2=0.78$ . The equations of these correlations are as below:

$$V_{p24} = -256.62 n + 6098.8 \quad r^2=0.86 \quad (5)$$

$$V_{p80} = -278.59 n + 5860.2 \quad r^2=0.78 \quad (6)$$

The determination coefficients showed that the diameter of 24 mm is the most reliable for estimating the  $V_p$  from  $n$  than other diameters.

The plot of the  $V_s$  as a function of the  $n$  for different diameters size is shown in figure 11. The highest determination coefficient,  $r^2=0.83$ , was obtained for the specimen diameter of 40 mm and the lowest was for the diameter of 54 mm with  $r^2=0.77$ . The equations of these correlations are as below:

$$V_{s40} = -121.67 n + 3095 \quad r^2=0.83 \quad (7)$$

$$V_{s54} = -98.516 n + 2819.7 \quad r^2=0.77 \quad (8)$$

In figure 12, the correlations of  $E$  with  $n$  are presented for different diameters size. In these correlations, the highest determination coefficient,  $r^2=0.88$ , was obtained for the specimen diameter of 24 mm and the lowest was for the diameter of 80 mm with  $r^2=0.82$ . The equations of these correlations are as below:

$$E_{24} = -5.105 n + 71.578 \quad r^2=0.88 \quad (9)$$

$$E_{80} = -4.5246 n + 57.024 \quad r^2=0.82 \quad (10)$$

In figure 13, the correlations of  $v$  with  $n$  are presented for different diameters size. As seen from the these figure, in all cases, due to inappropriate distribution of data, there is no meaningful relationship between  $v$  with  $n$ , and their correlations have the poor determination coefficients ( $r^2 < 0.45$ ).

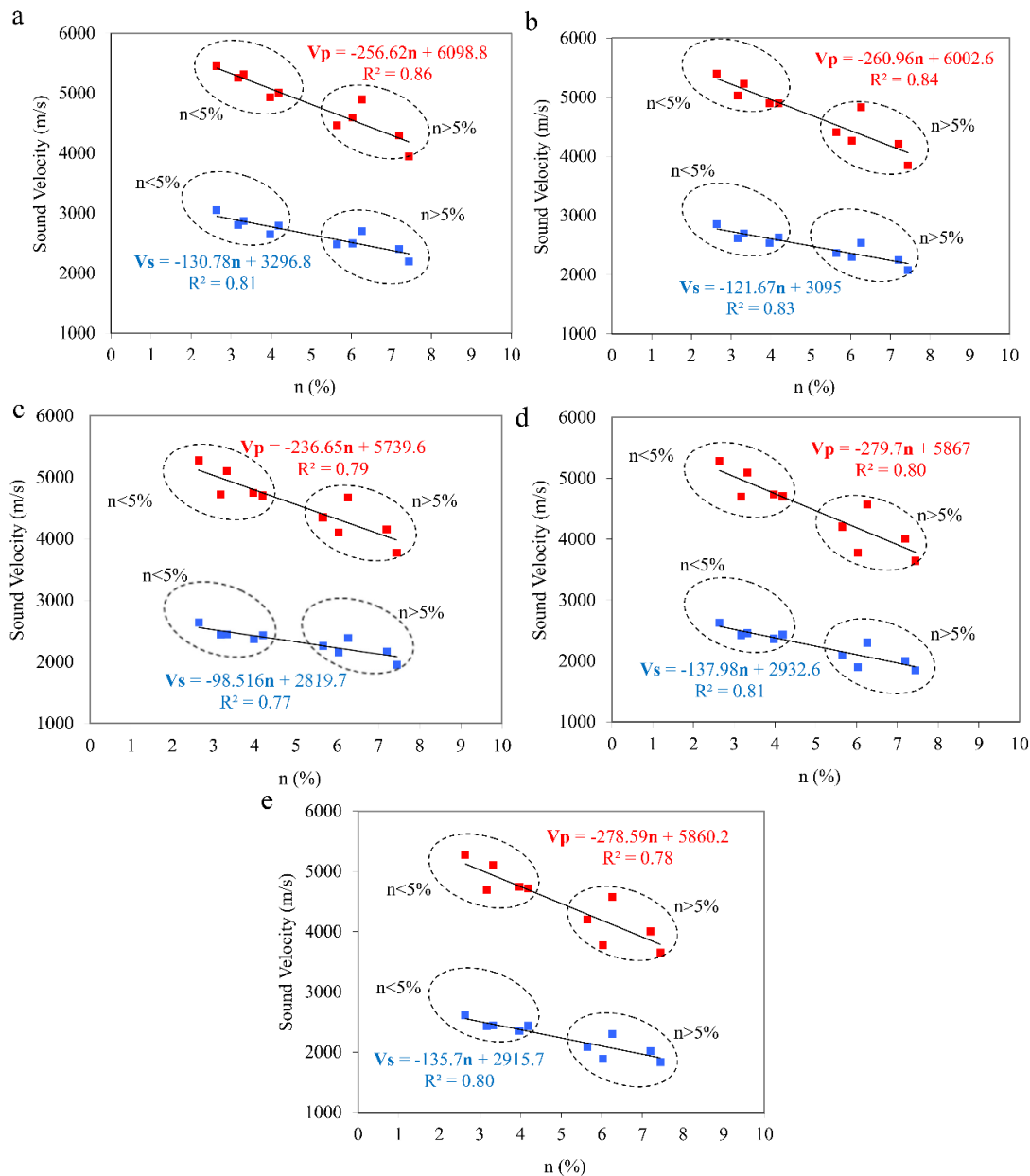


**Figure 11.** The correlation between Vp and Vs with n at different diameters size a: 24 mm, b: 40 mm, c: 54 mm, d: 68 mm, e: 80 mm

To investigate the validity of the regression equations in this study, t test was conducted among the achieved equations using the SPSS statistical package version 19. Here, only Eqs. 5, 7 and 9 that have the highest determination coefficients are used for t test.

The significance of the r values can be determined by t test, assuming that both variables are normally distributed and the observations are chosen randomly. The test compares the computed t-value with a tabulated t-value using the null hypothesis. In this study, a 95 % level of confidence was chosen. If the computed t-value is greater than the tabulated t-value, the null hypothesis is rejected. This means that r is significant. If the computed t-value is less than the tabulated t-value, the null hypothesis is not rejected. In this case, r is not significant. It can be seen from Table 5 that all of the computed t-values are greater than the tabulated t-values. Thus, it is concluded that there are real correlations between Vp, Vs and E with n.

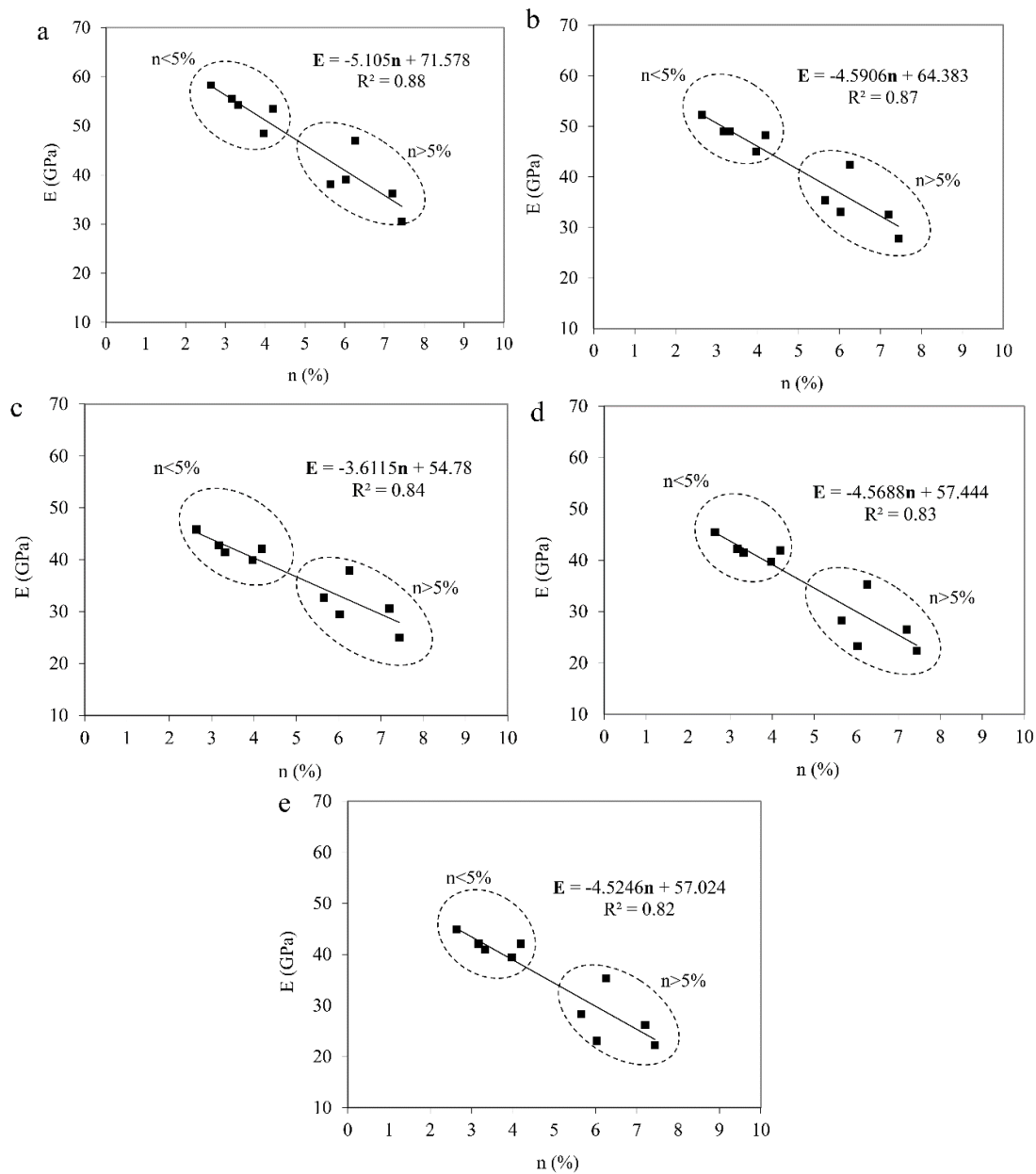


**Figure 12.** The correlation between E and n at different diameters size a: 24 mm, b: 40 mm, c: 54 mm, d: 68 mm, e: 80 mm

**Table 5.** Summarized the regression analyses results

Equation number	Regression equations	Determination coefficient ( $r^2$ )	t test	
			Calculated value	Tabulated value
5	$V_{p24} = -256.62n + 6098.8$	0.86	22.18	$\pm 2.262$
7	$V_{s40} = -121.67n + 3095$	0.83	20.36	$\pm 2.262$
9	$E_{24} = -5.105n + 71.578$	0.88	17.87	$\pm 2.262$

Although the determination coefficients of the Eqs. 5, 7 and 9 are 0.86, 83 and 0.88, respectively, and these are the very good values, it does not identify the valid equations necessarily. The correlation equations obtained in this study were evaluated by comparing their results with each other. The estimated values of  $V_p$ ,  $V_s$  and E by correlation equations shown in Table 5 were then plotted versus the measured values using 1:1 slope line (Figs. 14-16).

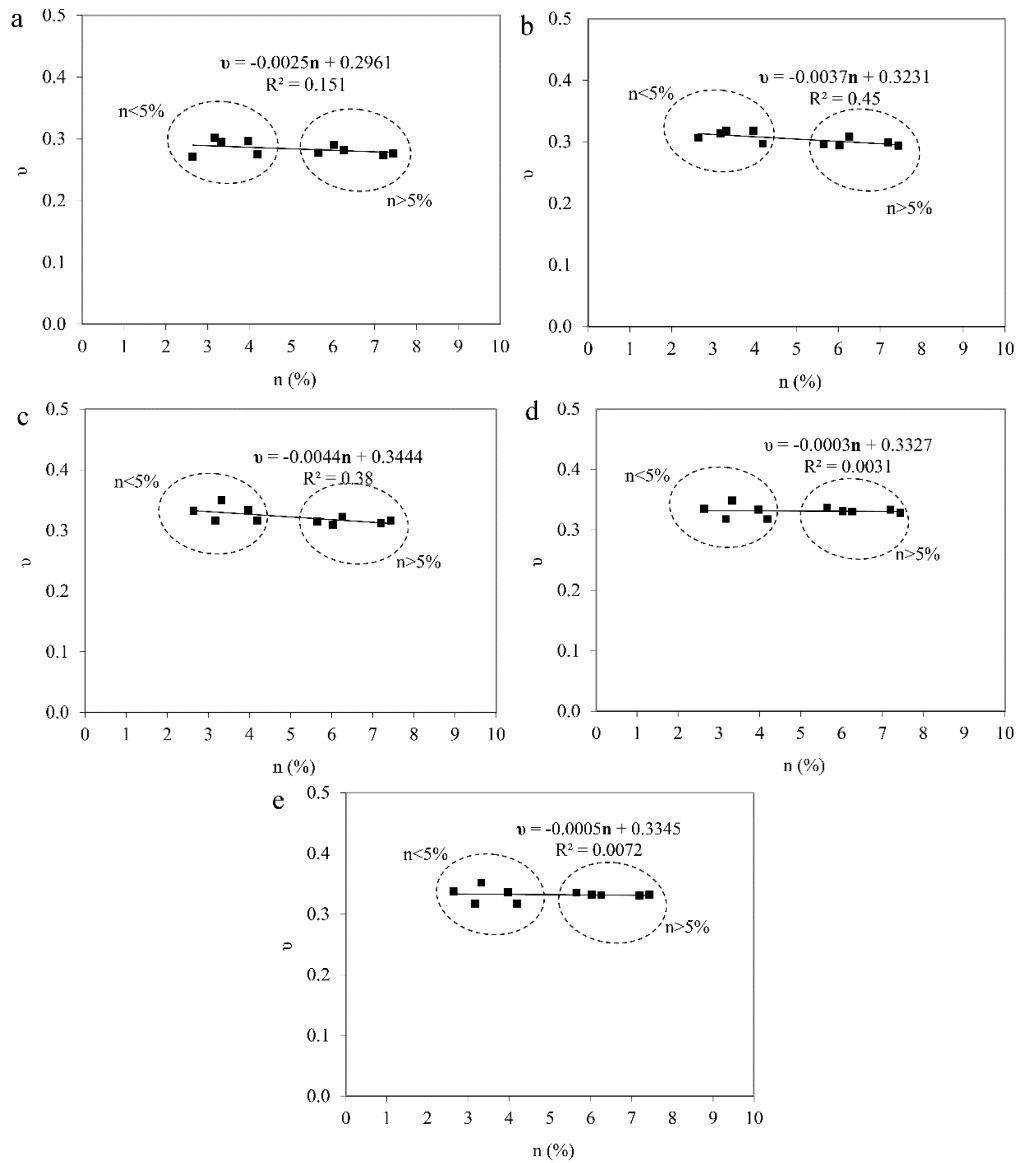


**Figure 13.** The correlation between  $v$  and  $n$  at different diameters size a: 24 mm, b: 40 mm, c: 54 mm, d: 68 mm, e: 80 mm

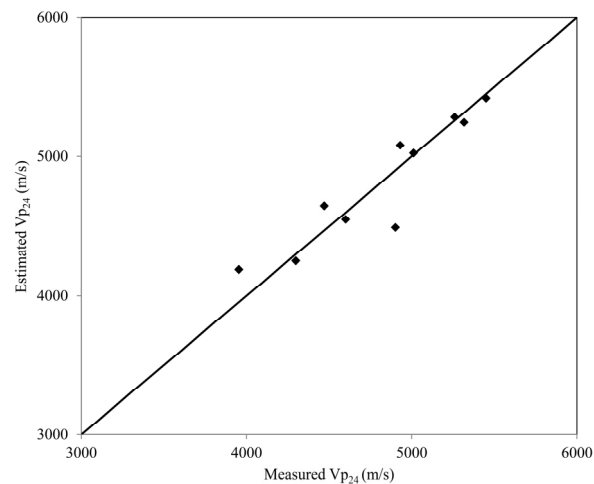


**Figure 14.** Measured  $V_p$  versus Estimated  $V_p$  from Eq. 5

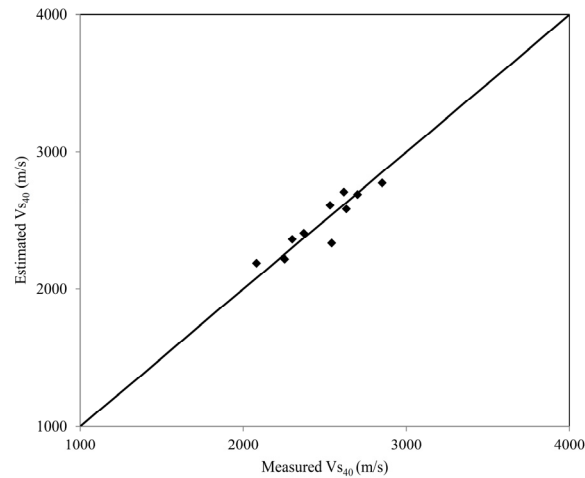


**Figure 15.** Measured Vs versus Estimated Vs from Eq. 7

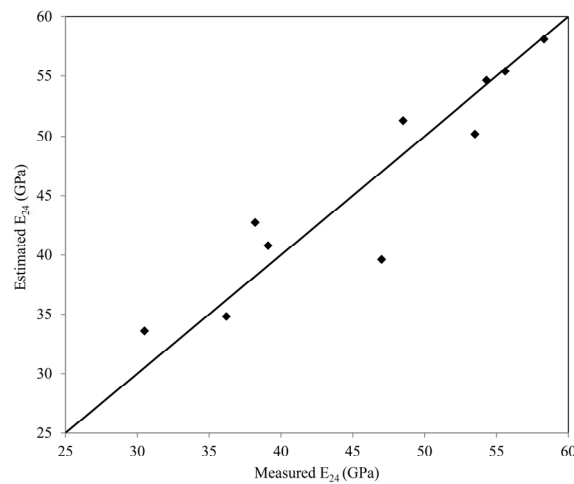


**Figure 16.** Measured E versus Estimated E from Eq. 9

A point lying on the line indicates an exact estimation. The figures indicate that the data points fall close to the 1:1 slope line and are scattered uniformly around it, suggesting that Eqs. 5, 7 and 9 with the associated coefficients are appropriate for estimating the  $V_p$ ,  $V_s$  and  $E$ , respectively.

## Conclusions

In this study, influence of specimen diameter size on the  $V_p$ ,  $V_s$ ,  $E$  and  $\nu$  was evaluated using specimens with diameters size 24, 40, 54, 68 and 80 mm. The correlations between the  $E$  and  $\nu$  with  $V_p$  and  $V_s$ , at different diameters size, were also investigated for 10 sandstone samples. Based on the findings presented, the main conclusions can be drawn;

According to classification of rocks using  $V_p$ , sandstones with respect to the diameters size of 24, 40, 54, 68 and 80 mm fall into the different rocks class with moderate, high and very high velocity.

Decrease in  $V_p$ ,  $V_s$ ,  $E$  and  $\nu$  values with increase diameter size is initially very significant and reaching a constant value at a Critical Diameter Size (CDS). The results showed that CDS is 54 and 68 mm for the sandstones with less porous (porosity < 5%) and porous (porosity > 5%), respectively.

The results showed that  $n$  is in good accuracy for estimating the  $V_p$ ,  $V_s$  and  $E$ , while there are no meaningful correlation between  $v$  with  $n$ .

The determination coefficients showed that the diameters size of 24, 40 and 24 mm are the most reliable for estimating the  $V_p$ ,  $V_s$  and  $E$  from  $n$ , respectively.

## References

- Al-Shayea, NA., 2004. Effects of testing methods and conditions on the elastic properties of limestone rock. *Eng. Geol.*, 74: 139-156.
- Ameen, MS., Smart, BG., Somerville, JM., Hammilton, S., Naji, NA., 2009. Predicting rock mechanical properties of carbonates from wireline logs (a case study: Arab-D reservoir, Ghawar field, Saudi Arabia). *Mar. Pet. Geol.*, 26: 430-444.
- Anon., 1979. Classification of rocks and soils for engineering geological mapping. part 1: Rock and soil materials. *Bull. Eng. Geo. Environ.*, 19: 355-371.
- Ayaz, Y., Kocamaz, AF., Karakoç, MB., 2015. Modeling of compressive strength and UPV of high-volume mineral-admixed concrete using rule-based M5 rule and tree model M5P classifiers. *Constr. Build. Mater.*, 94: 235-240.
- Brandes, HG., Robertson, IN., Johnson, GP., 2011. Soil and Rock Properties in a Young Volcanic Deposit on the Island of Hawaii. *J. Geotech. Geoenviron.*, 137 (6).
- Brotons, V., Tomas, R., Ivorra, S., Grediaga, A., 2014. Relationship between static and dynamic elastic modulus of calcarenite heated at different temperatures: the San Julians stone. *Bull. Eng. Geol. Environ.*, 73: 791-799.
- Christaras, B., Auger, F., Mosse, E., 1994. Determination of the moduli of elasticity of rocks. Comparison of the ultrasonic velocity and mechanical resonance frequency methods with direct static methods. *Mater. Struct.*, 27: 222-228.
- Ciccotti, M., Mulargia, E., 2004. Differences between static and dynamic elastic moduli of a typical seismogenic rock. *Geophys. J. Int.*, 157: 474-477.
- Eissa, EA., Kazi, A., 1988. Relation between static and dynamic Young's Moduli of rocks. *Int. J. Rock Mech. Min. Sci.*, 25: 479-482.
- Ercikdi, B., Karaman, K., Cihangir, F., Yılmaz, T., Aliyazıcıoğlu, S., Kesimal, A. 2016. Core size effect on the dry and saturated ultrasonic pulse velocity of limestone samples. *Ultrasonics* 72: 143-149.
- Ercikdi, B., Yılmaz, T., Kulekci, K., 2014. Strength and ultrasonic properties cemented paste backfill. *Ultrasonics* 54: 1386-1394.
- Eskisar, T., Altun, S., Kalıpcılar, I., 2015. Assessment of strength development and freeze-thaw performance of cement treated clays at different water contents. *Cold Reg. Sci. Technol.*, 111: 50-59.
- Fahy, MP., Guccione, MJ., 1979. Estimating strength of sandstone using petrographic thin-section data. *Bull. Eng. Geol. Environ.*, 16: 467-485.
- Fener, M., 2011. The Effect of Rock Sample Dimension on the P-Wave Velocity. *J. Nondestruct. Eval.*, 30: 99-105.
- Geological map of Khorramabad 1:25000., 2011. By Zamin Danesh-e-Pars consulting engineers.
- Hashemi, M., Bashiri Goudarzi, M., Jamshidi, A., 2018. Experimental investigation on the performance of Schmidt hammer test in durability assessment of carbonate building stones against freeze-thaw weathering. *Environ. Earth Sci.*, 77, 684.
- ISRM., 1981. Rock characterization testing and monitoring. ISRM suggested methods. In: Brown ET (ed), Pergamon Press, Oxford.
- Folk, RL., 1974. *Petrology of sedimentary rocks*. Hemphill, Austin, p 182
- Jamshidi, A., Torabi-Kaveh, M., 2020. Anisotropy in ultrasonic pulse velocity and dynamic elastic constants of laminated sandstone. *Q. J. Eng. Geol. Hydrogeol.*, 54(3): 1-9.
- Jamshidi, A., Torabi-Kaveh, M., Nikudel, MR., 2021. Effect of Anisotropy on the Strength and Brittleness Indices of Laminated Sandstone. *Iran. J. Sci. Technol. Trans. Sci.*, 45: 927-936.
- Jasinge, D., Ranjith, PG., Choi, SK., Kodikara, j., 2009. Mechanical Properties of Reconstituted Australian Black Coal. *J. Geotech. Geoenviron.*, 135 (7): 980-985.
- Ju, Y., Yang, Y., Peng, R., Lingtao Mao, L., 2013. Effects of Pore Structures on Static Mechanical Properties of Sandstone. *J. Geotech. Geoenviron.*, 139 (10): 435-442.

- Karaman, K., Kaya, A., Kesimal, A., 2015. Effect of the specimen length on ultrasonic Pwave velocity in some volcanic rocks and limestones. *J. Afr. Earth Sci.*, 112: 142-149.
- Khandelwal, M., Singh, TN., 2011. Predicting elastic properties of schistose rocks from unconfined strength using intelligent approach. *Arab. J. Geosc.*, 4: 435-442.
- King, M.S., 1983. Static and dynamic elastic properties of rocks from the canadian shield. *Int. J. Rock Mech. Min. Sci.*, 20: 237-241.
- Koncagül, E., Santi, P., 1999. Predicting the unconfined compressive strength of the Breathitt shale using slake durability, Shore hardness and rock structural properties. *Int. J. Rock Mech. Min. Sci.*, 36: 139-153.
- Martinez-Martinez, J., Benavente, D., Garcia-del-Cura, MA., 2012. Comparison of the static and dynamic elastic modulus in carbonate rocks. *Bull. Eng. Geol. Environ.*, 71: 263-268.
- Matula, M., Dearman, W.R., and Golodkovskaja, G.A., Pahl, A., Radbruch-Hall Dorothy, H., Sanejouand, R., 1979. Classification of rocks and soils for engineering geological mapping. part 1: Rock and soil materials. *Bull. Eng. Geo. Environ.*, 19: 364-371.
- Najibi, AR., Ghafoori, M., Lashkaripour, G.R., 2015. Empirical relations between strength and static and dynamic elastic properties of Asmari and Sarvak limestones, two main oil reservoirs in Iran. *J. Pet. Sci. Eng.*, 126: 78-82.
- Ocak, I., Seker, SE., 2012. Estimation of Elastic Modulus of Intact Rocks by Artificial Neural Network. *Rock Mech. Rock Eng.*, 45: 1047-1054.
- Özkan, I., Yayla, Z. 2016. Evaluation of correlation between physical properties and ultrasonic pulse velocity of fired clay samples. *Ultrasonics* 66: 4-10.
- Poulton, MM., Sternberg, BK., Farmer, I.W., 1991. In Situ Strength Measurements of Weak Rocks. *J. Geotech. Eng.*, 117 (9):11-20.
- Roshan, H., Masoumi, H., Zhang, Y., Al-Yaseri, AZ., 2018. Microstructural Effects on Mechanical Properties of Shaly Sandstone. *J. Geotech. Geoenviron.*, 144 (2): 11-25.
- Shakoor, A., Bonelli, RE., 1991. Relationship between petrographic characteristics, engineering index properties and mechanical properties of selected sandstones. *Bull. Eng. Geol. Environ.*, 28: 55-71.
- Ulusay, R., Tureli, K., Ider, MH., 1994. Prediction of engineering properties of a selected litharenite sandstone from its petrographic characteristics using correlation and multivariate statistical techniques. *Eng. Geol.*, 37: 135-157.
- Vasconcelos, G., Lourenço, PB., Alves, CAS., Pamplona, J., 2008. Ultrasonic evaluation of the physical and mechanical properties of granites. *Ultrasonics* 48: 453-466.
- Wua, D., Zhang, Y., Liu, Y., 2016. Mechanical performance and ultrasonic properties of cemented gangue backfill with admixture of fly ash. *Ultrasonics* 64: 89-96.
- Yagiz, S., 2011. P-wave velocity test for the assessment of some geotechnical properties of rock materials. *Bull. Mater. Sci.*, 34: 943-957.
- Yilmaz, I., 2007. Differences in the geotechnical properties of two types of gypsum: alabastrine and porphyritic. *Bull. Eng. Geol. Environ.*, 66: 187-195.
- Yilmaz, T., Ercikdi, B., Karaman, K., Kulekci, G., 2014. Assessment of strength properties of cemented paste backfill by ultrasonic pulse velocity test. *Ultrasonics* 54: 1386-1394.
- Zalooli, A., Khamehchiyan, M., Nikudel, M.R., Jamshidi, A., 2017. Deterioration of travertine samples due to magnesium sulfate crystallization pressure: examples from Iran. *Geotech. Geol. Eng.*, 35(1): 463-473.

